Non Linear Analysis Of Rubber Boot Sear

Shashikanth. C and K. Mahesh Dutt.

Abstract—This rubber boot seal project demonstrates geometric nonlinearities (large strain and large deformation), nonlinear material behavior (rubber), and changing status nonlinearities (contact). The objective of this project is to show the advantages of the surface-projection-based contact method and to determine the displacement behavior of the rubber boot seal, stress results, and location of the contact point on the outer surface and inner surface of the boot during the shaft motion

A rubber boot seal with half symmetry is considered for this analysis. There are three contact pairs defined one is rigid-flexible contact between the rubber boot and cylindrical shaft, and the remaining two are self-contact pairs on the inside and outside surfaces of the boot. The problem is solved in three load steps:

1. ***Initial interference between the cylinder and boot.***
2. ***Vertical displacement of the cylinder (axial compression in the rubber boot).***
3. ***Rotation of the cylinder (bending of the rubber boot).***

Key words: FEM, rubber boot seal analysis.

I. INTRODUCTION

Rubber boot seals are used in many industrial applications to protect the flexible joint between two bodies. In the automotive industry, rubber boot seals cover constant velocity joints on the drive shaft to protect them from the outside elements (dust, humidity, mud, etc.). These rubber boots are designed to accommodate the maximum possible swing angle of the joints and to compensate for changes in the shaft length.

Rubber seals are mechanical seals widely used in both dynamic as well as static sealing applications to prevent fluid leakage between two mating surfaces and to cover and protect the moving parts. These seals are generally made from natural and synthetic elastomers. The flexible nature of the seals, unlike adhesives, makes them ideal for use in a number of industries, including construction, automotive, and aerospace. Other prominent features of rubber seals that have led to their widespread adoption is the resistance to aging and adequate flame retardation ability.

Shashikanth.C., PG Scholor, Dept. ofmechanical engineering, K.S Instituite of Technology, VTU, Bangalore, India.,

K,MaheshDutt., Asst. Prof., Deptt. Of mechanical engineering, K.S Institute of Technology, VTU, Bangalore, India.

II. RUBBER BOOT SEAL ANALYSIS

A. Modeling:

Due to the symmetry of the structure, only half of the rubber boot is modeled. For the rubber boot, the hyper elastic material model is used. The shaft is considered as a rigid body. Modeling this problem involves the following tasks:

- Model the rubber boot seal
- FE model generation

B. Modeling Rubber Boot

The modeling is done using CATIA V5 and is modeled as a solid body. Due to having symmetry in the structure of the rubber boot seal only half symmetric model is made.

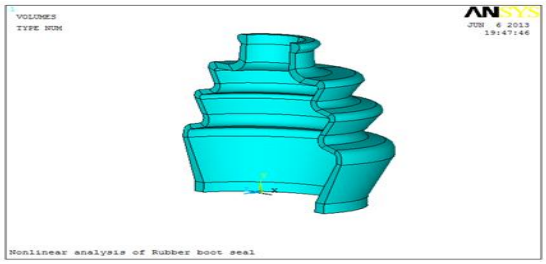

Fig 1: 3D model of rubber boot seal.

C. Fe Model Generation:

Here we are generating the finite element model and then defining the element type, material properties and contacts to the problem.

The solid model of rubber boot is meshed using 8 node hexahedral element with global element size 2. Because of having symmetry the meshing is achieved by using sweep method. And the shaft is made as the rigid body here by modeling it in hyper mesh.

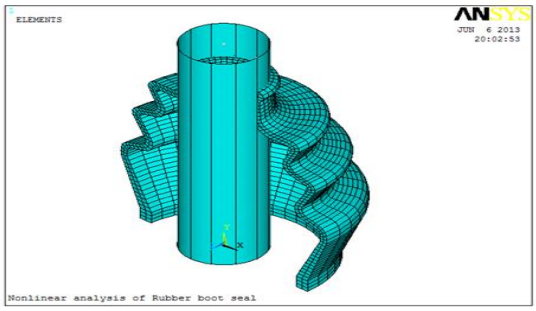

Fig2: FE model Rubber boot seal (Solid mesh).

D. Defining element type:

The solid hexahedral element of rubber boot seal is defined using Solid 185. This model has 3387 elements.

E. Solid 185 Element description:

SOLID185 is used for 3-D modeling of solid structures. It is defined by eight nodes having three degrees of freedom at each node: translations in the nodal x, y, and z directions. The element has plasticity, hyper elasticity, stress stiffening, creep, large deflection, and large strain capabilities. It also has mixed formulation capability for simulating deformations of nearly incompressible elasto-plastic materials, and fully incompressible hyper elastic materials. As for our analysis, solid 185 is selected to support large deflection, hyper elasticity as we are dealing with rubber, and large strain capabilities.

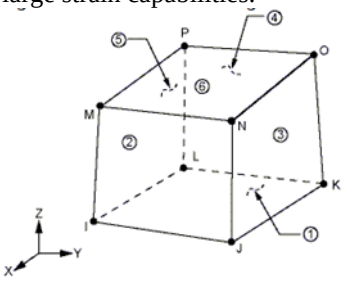

Fig3:Solid 185 hexahedral element plot

F. Defining material properties:

Here we have defined rubber properties in terms of Neo-Hookean material model for boot seal. The material properties are given below. Where mu is the initial shearing modulus developed in the material during compression. And d is incompressibility parameter of the the rubber material constant.

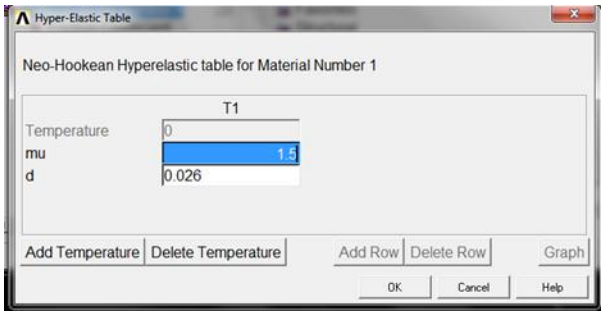

Fig4: material properties of neo-hookean model

Along with this the friction co-efficient value also we have defined as the surfaces of boot seal will come in contact with itself during compression provided by the gear shifting shaft. So a fiction co-efficient value of 0.2 is defined, which is for the boot seal materials.

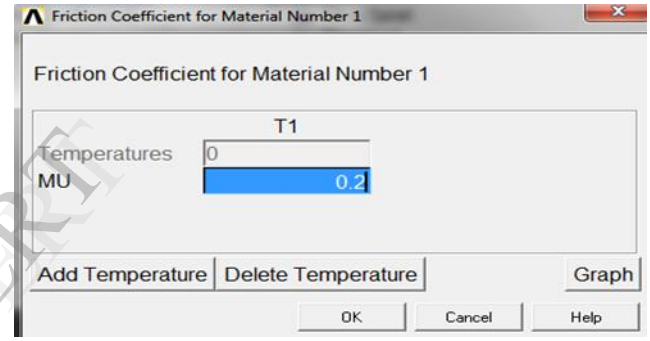

Fig5: coefficient of friction of neo-hookean model.

G. Defining contacts:

When two separate surfaces touch each other such that they become mutually tangent, they are said to be in contact.

In the common physical sense, surfaces that are in contact have these characteristics:

- They do not interpenetrate.
- They can transmit compressive normal forces and tangential friction forces.
- They often do not transmit tensile normal forces.
- They are therefore free to separate and move away from each other.

Hence we can define contact as contact is a changing-status nonlinearity. That is, the stiffness of the system depends on the contact status, whether parts are touching or separated. So the contacts used here in our analysis are defines below. Three contact pairs are defined to simulate contact occurring in the rubber boot during the shaft movement:

- Rigid flexible contact between the rigid cylindrical shaft and the inner surface of the rubber boot.
- Self-contact at the inner surface of the rubber boot using the surface-projection-based contact method.
- Self-contact at the outer surface of the rubber boot using the surface-projection-based contact method.

1. Rigid-flexible Contact Pair between Rigid Shaft and Rubber Boot

The rigid cylindrical shaft is modeled by the Target 170 element with the TSHAP,CYLI command. The radius of the cylindrical shaft is 14 mm. This rigid cylinder is in initial interference with the internal surface of the rubber boot.

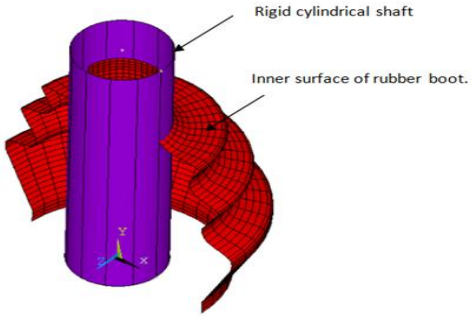

Fig6: rigid-flexible contact pair between rigid shaft and rubber boot

H. The following contact settings are used for the contact elements Contact 173:

KEYOPT (9) = 2 to include interference with ramped effects

KEYOPT (4) = 0 to set the location of the contact detection point at the gauss integration point.

Gauss integration point are the points in the elements where all stresses and strains are calculated and then hence extrapolated to the nodes and then to elements. Ramped Effect is the behavior where all the initial loads and boundary conditions applied in a linear incremental way.

I. About contact 173:

CONTA173 is used to represent contact and sliding between 3-D "target" surfaces TARGET 170 i.e. the shaft and a deformable surface i.e. Rubber boot seal, defined by this element. The element is applicable to 3-D structural.

Contact 173 Assumptions and restrictions:

The 3-D contact element must coincide with the external surface of the underlying solid or shell.

This element is nonlinear and requires a full Newton iterative solution, regardless of whether large or small deflections are specified.

The normal contact stiffness factor (FKN) must not be so large as to cause numerical instability.

You can use this element in nonlinear static or nonlinear full transient analyses. In addition, you can use it in modal analyses, buckling analyses, and harmonic analyses.

FKN- It is the stiffness created because of the contact pressure transformation between two bodies coming in contacts and these contact pressure acts in the direction normal to the contact status.

2. Self contact pairs at inner and outer surfaces of rubber boot

To model a self contacting pair, both the target and contact surfaces are the same. KEYOPT(4) = 3 is used to define surface-projection-based contact.

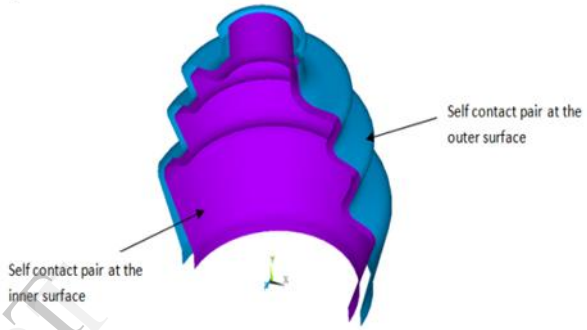

Fig7: Self contact pairs at inner and outer surfaces of rubber boot

AUTO command is used to set certain real constants and key options to recommended values in order to achieve better convergence based on overall contact pair behavior. This command affects the following key options for the contact elements (element type 4) used to define the self contact pairs:

KEYOPT (7) is modified from 0 to 1. This is recommended to prevent spurious contact for the self contact pairs, and it will speed up the contact searching for these pairs.

KEYOPT (10) is modified from 0 to 2 to allow contact stiffness to be updated at each iteration based on the underlying element stresses. For the majority of cases, the automatic setting of the contact stiffness will provide better convergence and accuracy of the analysis while preventing ill-conditioning of the global stiffness matrix.

The above two option modifications are the most important part of this analysis as the gear shifting shaft is continuously pressing the boot seal and hence there is continuous change in the stiffness of the boot seal, so to capture the continuous change in stiffness we need to set these option for these contacts.

Necessity of Self Contact on inner and outer surface is because when the rubber boot is compressed by shaft it get deforms and become in contacts with itself hence there is a change in stiffness the contact region where it

isgetting touched by itself, so to capture this stiffness change we are applying self contact here.

III. SOLUTIONS AND CONTROLS

A. Boundary conditions and load steps:

The model is constrained at the symmetry plane by restricting the out-of-plane translation. The bottom portion of the rubber boot is restricted in axial and radial directions. The load is applied in terms of displacements and rotations through different load steps.

Load step 1:

Base node at the end of shaft's centre axis is constrained in all direction. So that it is free to move and is allowed to have movement to compress the rubber with required distance. Also we have applied the symmetric boundary condition to boot seal as we have modeled half part.

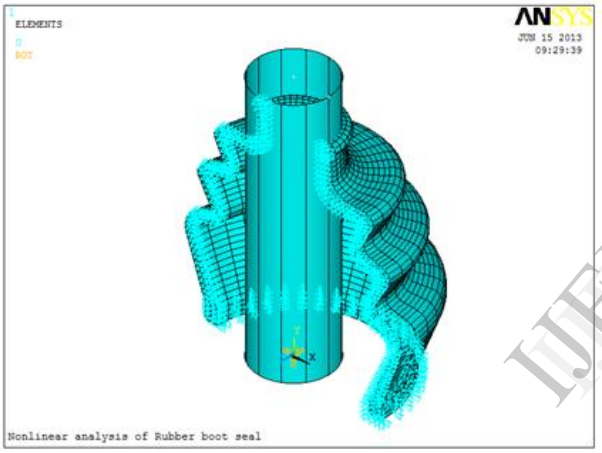

Fig8: Boundary conditions for 1nd load step.

So the above picture shows the 1st load step boundary conditions. In this load step we are not applying external load just only constraining the model for initial setup and making it to get converged with 5 sub steps.Solving this load step 1 gives the below graph. This the convergence graph for LC1 it takes around 12 iterations to get converged in total time of 1 second.

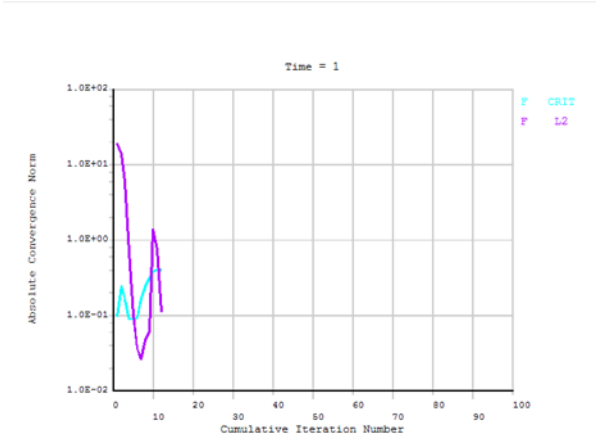

Fig9:The convergence plots for load step 1.

Load step 2:

Boot seal gets compressed when the shaft moves down. The vertical movement of the shaft is governed by the displacement applied to the base node at the end of the shaft's centre axis. The displacement applied here is 10mm downward Y axis. No. of sub step we have considered is 10, it means we are dividing our 2nd load step into 10 parts to achieve easy convergence.

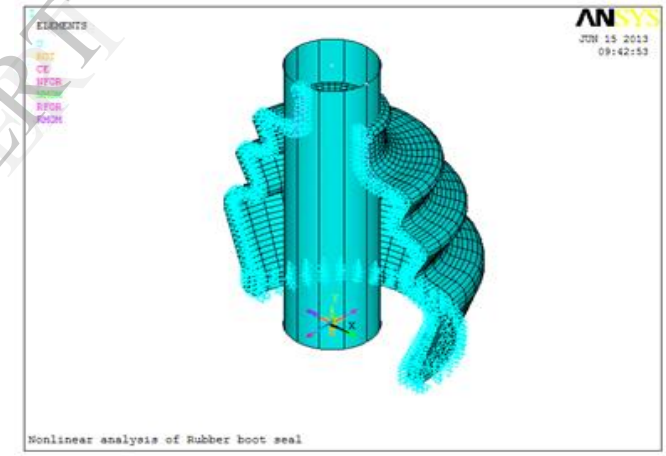

Fig10: Boundary conditions for 2nd load step.

The bottom node of the shaft is made to move down by 10mm and by doing this the boot seal is getting compressed as all parts are in contacts.

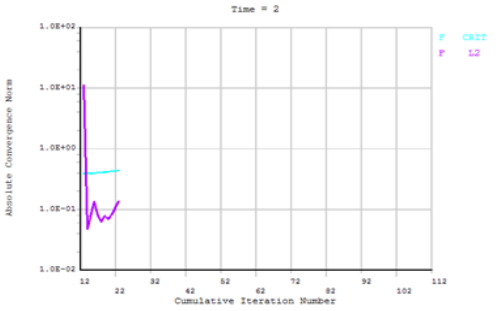

Fig11: The convergence plot for load step 2

Here 23 iteration are done to achieve convergence in total time of next 1 second and this LC is continued after the end of 1 second.

Load step3:

Shaft is rotated by giving certain amount of rotation about z-axis to the base node (pilot node) at the end of the shaft's centre axis. The rotation is made about Z axis by an angle of 55 degree. This will continue after 1st and 2nd LC.The boundary condition list is given below.

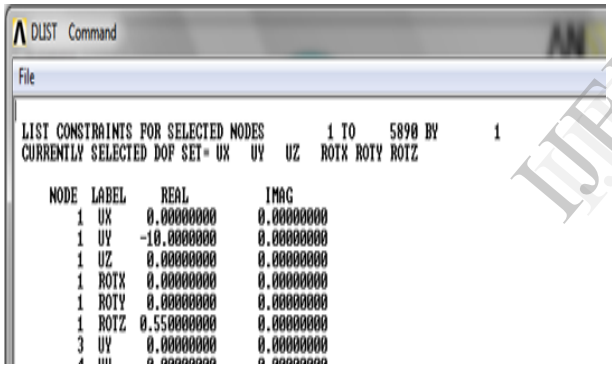

Fig12:Boundary conditions

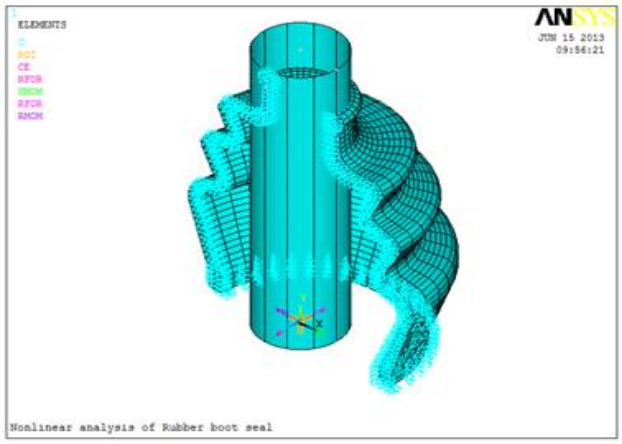

Fig13: Boundary conditions for 2nd load step.

In this load step we gave defined 20 sub step and time defined for this LC is 1 second which is the continuation after LC1 and2. This LC is taking 214 iterations to get converged.

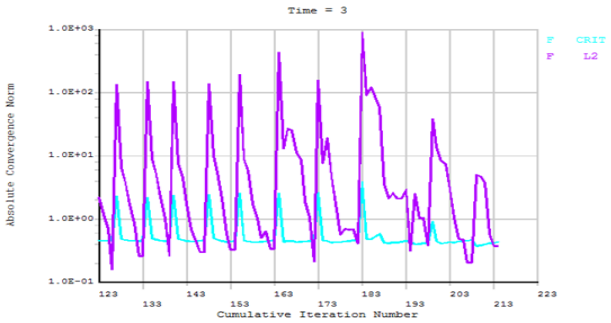

Fig14: The convergence plot for load step 3

In all above graphs Blue colour line is the Force Convergence and purple colour is the internal force generating and trying to get converged and becoming in equilibrium with the Blue colour line.

B. Solution method used:

For this analysis we have opted for Newton-Raphson method, this method brings down the external load we have applied in equilibrium to the internal load developed during solving.

Initially from the external load applied to the structure and using stiffness matrix it calculate the internal displacements from which the solver calculates the internal load, and thus this method compares the both loads if they are in equilibrium than solver understands that the problem is get converged if not then proceeds for next iteration with the calculated internal load as external load, this process continues till the solver achieves the equilibrium.

C. Analysis and solution controls:

A nonlinear static analysis is performed in three load steps. Large-deflection effects are included in the analysis.

Large deflection effect we are including because the problem is having geometric non linearity which mean with application of small displacement or force the structure is going to have very large strains but these strain are in elastic limits. Here the stiffness is varying constantly as the forces are not proportional to the displacement in the structure hence changing stiffness and influence of Non- linearity.

Stiffness(k)=(force applied at any point)/(displacement at that point)

Here we can notice the changing stiffness status during geometric Non linearity's.We are comparing the results obtained by using contacts method at different contact detection schemes, we have considered 3N/mm as contact stiffness we have used surface to surface contact method and putting the above stiffness value. A total time of 3 seconds is considered for solution.

Thus checking the solving time or convergence time at different contact detection schemes. Those are at

1. Gauss points
2. Nodal point
3. Element or surface.

Gauss Points: These are the integration points where solver calculates all the stress and strain values. In Finite Element Analysis (FEA) the simulation results are managed in so called integration points. Integration points are used to control and monitor values inside of a finite element.Integration points are located within a finite element and therefore strongly connected to them. The position of an integration point inside a finite element is based on the quadrature and the integration method (gauss, Newton-cotes).

Nodal point: The results at nodal points are the extrapolation of the results obtained at gauss points.

Element or Surface: From field variables at nodal points using the shape function all other variables are then calculated within an element.

So, Figure and Table Simulation statistics for different contact detection method illustrate the following advantages of the surface-projection-based contact method by comparing it with other available contact detection algorithms.

Compared to other methods, the surface-projection-based contact method (KEYOPT (4) = 3) requires the least number of cumulative iterations to solve this problem.

Convergence of the problem is less sensitive to the normal contact stiffness factor (FKN) when using the surface-projection-based contact method (KEYOPT (4) =3).

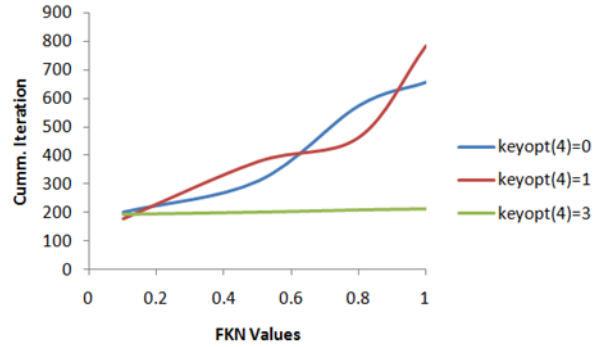

Fig16: Comparison of cumulative iterations for different contact detection methods

The surface-projection-based contact method produces smoother contact forces than other contact detection algorithms. It is less sensitive to the magnitude of the contact stiffness.

	KEYOPT(4) =0; Gauss Point	**KEYOPT(4) =1; Nodal Point**	**KEYOPT(4) =3; Surface Projection**
Sub steps	57	70	25
Cumulative Iterations	655	784	214
Simulation Time (sec)	3265	3851	1044

In general, the surface-projection-based contact method is much more expensive in computational time. In this particular model, the total number of iterations and sub steps used with this method is much less than in other contact detection algorithms. The overall performance using the surface projection method turns out to be much better. This can be observed in the table below:

Simulation statistics for different contact detection methods

IV. RESULTS AND DISCUSSIONS

A. Displacement plot:

The maximum deformation in the rubber boot seal is 56.2254 mm

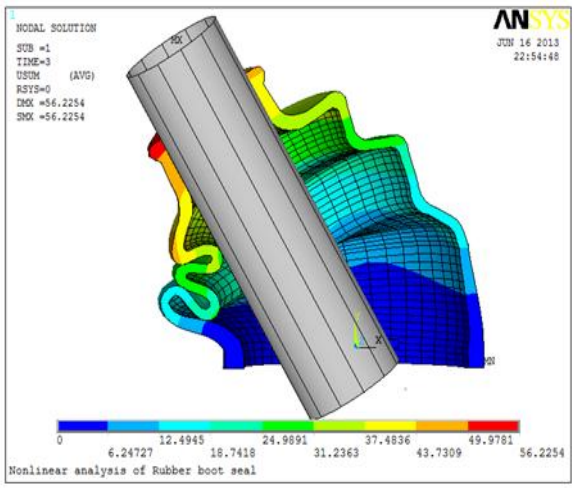

Fig17: Displacement plot

B. The stress in the rubber boot seal:

The maximum stress in the rubber seal is 1.11184 MPa

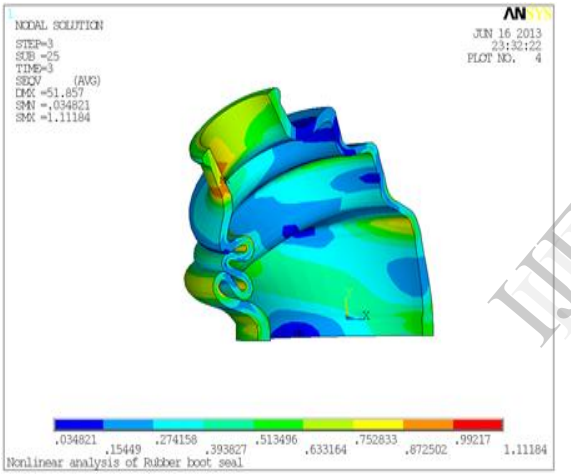

Fig18: stress in the rubber boot seal

The force and moment generated due to compression at different time:

Time in s	Force in N	Moment in N-mm
0.1	-1.51482	-6.65E-05
0.2	-3.07181	-1.31E-04
0.3	-4.49275	-1.92E-04
0.4	-5.83288	-2.65E-04
0.5	-7.16725	-3.42E-04
0.6	-8.40628	-4.15E-04
0.7	-9.54121	-4.94E-04
0.8	-10.6452	-5.83E-04
0.9	-11.7149	-6.69E-04
1	-12.6803	-7.45E-04
1.1	-12.6112	-7.61E-04
1.2	-12.6466	-7.56E-04
1.3	-12.6151	-7.59E-04
1.4	-12.6356	-7.59E-04
1.5	-12.6354	-7.59E-04
1.6	-12.6356	-7.59E-04
1.7	-12.6355	-7.59E-04
1.8	-12.6355	-7.59E-04
1.9	-12.6355	-7.59E-04
2	-12.6355	-7.59E-04
2.05	-16.0265	221.979
2.1	-12.5462	182.079
2.15	-12.4457	227.099
2.2	-12.6842	316.432
2.25	-12.542	413.628
2.3	-12.4832	527.978
2.35	-12.7981	580.733
2.4	-12.7448	665.313
2.45	-13.0886	731.593
2.5	-13.2484	861.22
2.55	-13.4156	1015.68
2.6	-14.218	1089.39
2.65	-14.4452	1177.28
2.7	-16.0328	1249.88
2.75	-15.0611	1356.93
2.8	-15.1446	1425.03
2.85	-15.7431	1533.71
2.9	-16.242	1610.56
2.95	-18.2392	1844.84
3	-18.4441	1783.51

A total of 18.4441 N of force is generated in the rubber seal when compressed fully. The maximum of 1799.51 N-mm moments is produced when compressed fully.

Force v/s time graph and moment v/s time graph:

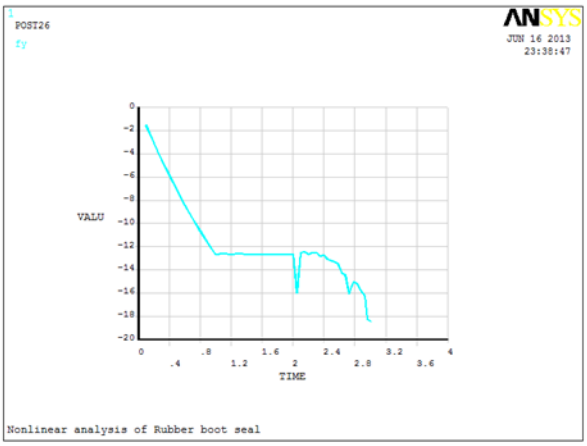

Fig19: force v/s time graph

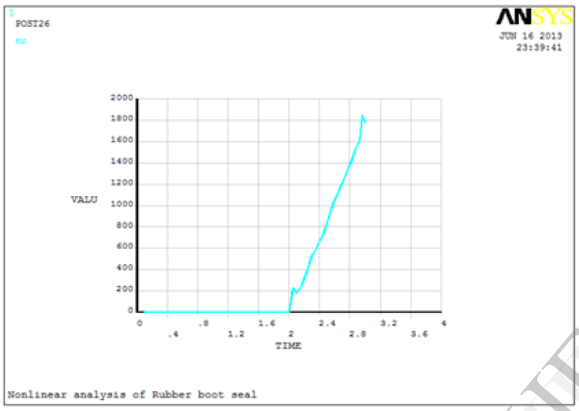

Fig20: moment v/s time graph

Elastic strains in x, y and z directions:

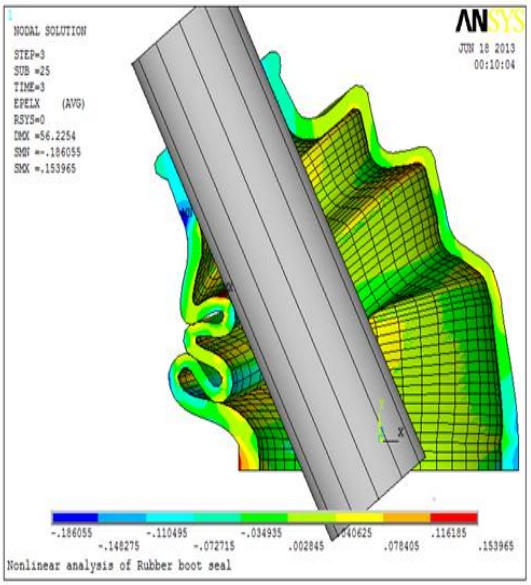

Fig21: Strain in x direction

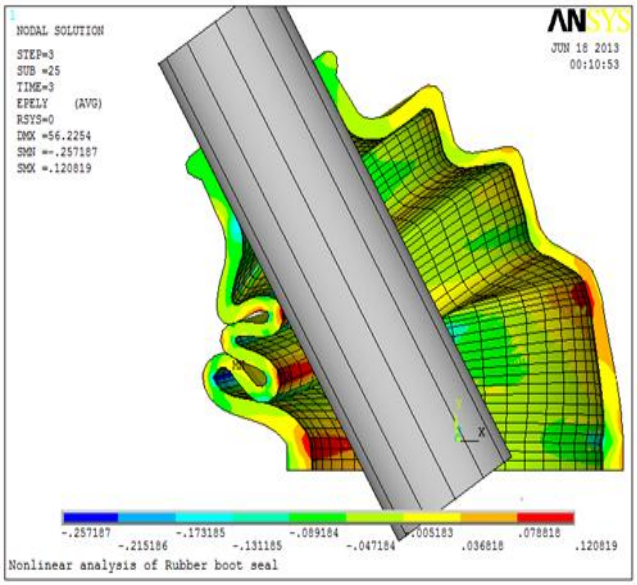

Fig22: Strain in y direction

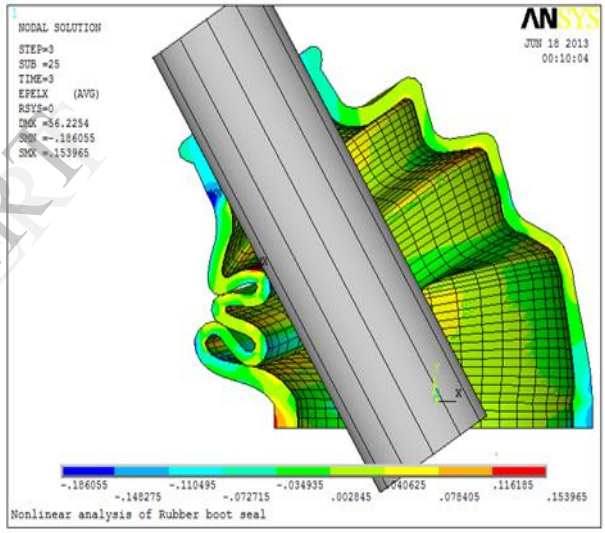

Fig23: Strain in z direction

C. Comparison and validation of ANSYS results with the test results:

Time in s	ANSYS Force in N	Testing force in N	ANSYS Moment in N-mm	Testing moment in N-mm
0.1	-1.51482	-1.35	-6.65E-05	-6.41E-05
0.2	-3.07181	-2.95	-1.31E-04	-1.22E-04
0.3	-4.49275	-4.32	-1.92E-04	-1.97E-04
0.4	-5.83288	-5.78	-2.65E-04	-2.65E-04
0.5	-7.16725	-7.01	-3.42E-04	-3.42E-04
0.6	-8.40628	-8.53	-4.15E-04	-4.34E-04
0.7	-9.54121	-9.39	-4.94E-04	-4.85E-04
0.8	-10.6452	-10.48	-5.83E-04	-5.88E-04
0.9	-11.7149	-11.76	-6.69E-04	-6.52E-04
1	-12.6803	-12.72	-7.45E-04	-7.20E-04

1.1	-12.6112	-12.55	-7.61E-04	-7.31E-04
1.2	-12.6466	-12.61	-7.56E-04	-7.64E-04
1.3	-12.6151	-12.75	-7.59E-04	-7.49E-04
1.4	-12.6356	-12.69	-7.59E-04	-7.41E-04
1.5	-12.6354	-12.58	-7.59E-04	-7.44E-04
1.6	-12.6356	-12.62	-7.59E-04	-7.43E-04
1.7	-12.6355	-12.6	-7.59E-04	-7.42E-04
1.8	-12.6355	-12.64	-7.59E-04	-7.45E-04
1.9	-12.6355	-12.58	-7.59E-04	-7.50E-04
2	-12.6355	-12.64	-7.59E-04	-7.51E-04
2.05	-16.0265	-15.24	221.979	212.647
2.1	-12.5462	-12.59	182.079	167.534
2.15	-12.4457	-12.31	227.099	218.876
2.2	-12.6842	-12.58	316.432	303.567
2.25	-12.542	-12.44	413.628	401.547
2.3	-12.4832	-12.5	527.978	514.468
2.35	-12.7981	-12.7	580.733	565.768
2.4	-12.7448	-12.85	665.313	659.536
2.45	-13.0886	-13.22	731.593	720.674
2.5	-13.2484	-13.24	861.22	847.784
2.55	-13.4156	-13.55	1015.68	1006.897
2.6	-14.218	-14.23	1089.39	1070.564
2.65	-14.4452	-14.42	1177.28	1170.567
2.7	-16.0328	-15.67	1249.88	1236.765
2.75	-15.0611	-15.01	1356.93	1342.655
2.8	-15.1446	-15.11	1425.03	1414.785
2.85	-15.7431	-15.81	1533.71	1540.765
2.9	-16.242	-16.22	1610.56	1597.566
2.95	-18.2392	-17.86	1844.84	1842.675
3	-18.4441	-18.12	1783.51	1822.546

Graphs comparing the testing results and ANSYS results:

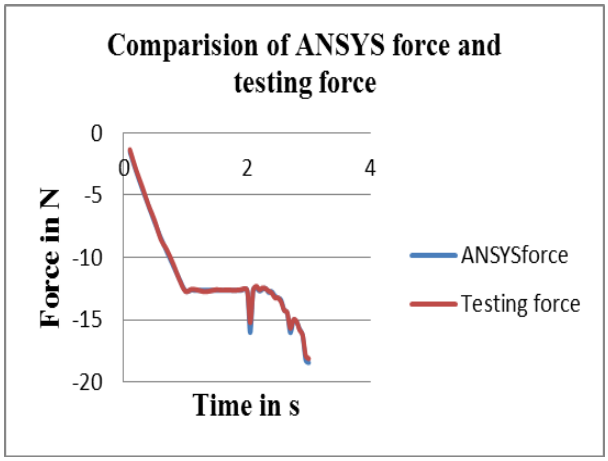

Fig23: Graph comparing testing and ANSYS forces.

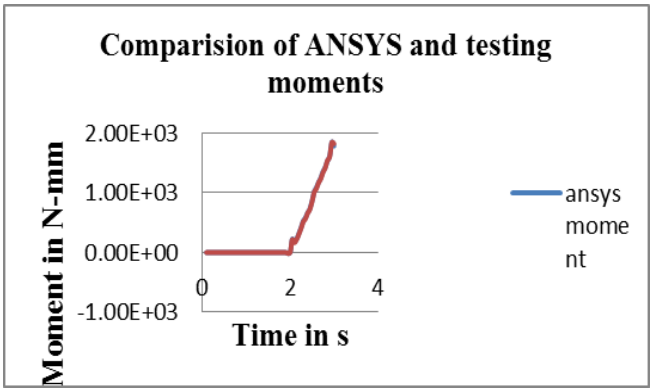

Fig24: Graph comparing testing and ANSYS moments.

V. Conclusion

The project is to show the advantages of the surface-projection-based contact method and to determine the displacement behavior of the rubber boot seal, stress results, and location of the contact point on the outer surface and inner surface of the boot during the shaft motion

Contact points means how a part of rubber is coming in contacts with itself hence capturing the changing stiffness. As the contacts are spontaneous and are changing instantly

Compared to other methods (gauss point and nodal point) , the surface-projection-based contact method requires the least number of cumulative iterations to solve this problem.

As the cumulative iterations are less for surface projection based method the computational time for solving the problem is less.

In stress plot of rubber boot the location of the critical zones where the maximum stress occurs in the boot at maximum shaft angle. In spite of the fact that it is low, and considering the fatigue effects of the material after a given number of cycles, it is clear that these areas are the most likely to fail under fatigue loads.

At the end of the analysis the force generated are less and the moments are high. Forces are less because rubber has high volumetric compressibility and hence tendency to absorb most of the force generated so that rubber boot has its motion smoothly,

With the maximum compression we can see the von mises is only 1.11184 Mpa only means it can handle more force without failure also shows the properties of rubbers are good enough for sustaining a longer life.

Surface-projection-based is not used to define contact between the rigid shaft and the rubber boot because this method does not support rigid surfaces defined by primitive target segments.

This analysis gives results with ease than that achieved in lab test.

VI. REFERENCES

[1]Faguo Sun, Tianxiang Yu, Weimin Cui, Xiao Zong, " TheSeal Reliability Analysis of Oring Seals", IEEE, 2009

[2] G. Rio, H. Laurent, G. Ble`s, "Asynchronous interface between a finite element commercial softwareABAQUS and an academic research code HEREZH++", France, march 2008

[3] Peter A.A, Van Hoogstraten, "A Eulerian approach to the finite element modelling of neo-hookean rubber material", Institute of Vervolgopleidingen, TUE.

[4] Davia.W, Nicholson and Norman.W.Nelson, "Finate element analysis in designwith rubber",Stevens Institute of Technologies,Hoboken, New Jersey.

[5] Grama R. Bhashyam, "ANSYS mechanical-a powerful nonlinear simulation tool", September 2002.

[6] Leandro Jaskulski, "Driveshaft Seal Boot Finite Element Analysis".AlbarusTransmissõesHomocinéticas ltda. Porto Alegre, R.S., Brazil

[7] Seung-Bum Kwak , Nak-Sam Choi,"Micro-damage formation of a rubber hose assembly for automotive hydraulic brakes under a durability test", Science direct, 2009.

[8] MSE software corporation, "Nonlinear analysis of elestomers", technical papers.

[9] Akash.A.Vandakudri, Dr.K.S.Krishnamurthy, "Elastomer Applications In New Age Industries And Engineering Support". A.Stenti ,D.Moens, P.Sas, W.Desmet,"

[10] A three-level non-deterministic modeling methodology for the NVH behavior of rubber connections", Journal of Sound and Vibration,2010.

[11] Mario D. Romero-Sanchez, M. Mercedes Pastor-Blas, Teresa delPilarFerrandiz-Gomez, Jose Miguel Martin-Martinez, "Durability of the halogenation in synthetic rubber", International Journal of Adhesion & Adhesives 21 (2001) 101-106.

[12] NándorBékési, "Modelling Friction and Abrasive Wear of Elastomers", Budapest University of Technology and Economics, Budapest, Hungary.